Oriented growth of multiple layered thin films of metal-organic frameworks (MOF-on-MOF)

Ken Ikigaki[a], Kenji Okada[a], Yasuaki Tokudome[a], Takashi Toyao[c], Paolo Falcaro[d], Christian J. Doonan*[e], and Masahide Takahashi*[a, b]

Abstract: Herein we report the precise alignment of multiple layers of metal-organic framework (MOF) thin films, or MOF-on-MOF films, over macroscopic length scales. The MOF-on-MOF films are fabricated by epitaxially matching the interface of each layer. The first MOF layer ($Cu_2(BPDC)_2$, BPDC = biphenyl-4,4'-dicarboxylate) is grown on an oriented metal hydroxide ($Cu(OH)_2$) film, that acts as a sacrificial substrate, via a 'one-pot' approach. Aligned second ($Cu_2(BDC)_2$, BDC = benzene 1,4-dicarboxylate, or $Cu_2(BPYDC)_2$, BPYDC = 2,2′-bipyridine-5,5′-dicarboxylate) and third ($Cu_2(NDC)_2$, NDC = naphthalene 2,6-dicarboxylate) MOF layers can be deposited using LPE (liquid phase epitaxy). The co-orientation of the MOF films is confirmed by X-ray diffraction and scanning electron microscopy. Importantly, our strategy allows for the synthesis of macroscopically aligned MOF films composed of organic linkers, e.g. $Cu_2(BPYDC)_2$, that cannot be readily grown on a $Cu(OH)_2$ surface. We show that aligned MOF films furnished with bipyridyl moieties facilitate the growth of Ag metal nanoparticles within the MOF lattice that show a unique anisotropic plasmon resonance; however, without such functionality the MOF-nanoparticle composites could not be formed. We show that the MOF-on-MOF approach expands the chemistry of heteroepitaxially oriented MOF films and provides a new toolbox for the preparation of multifunctional porous coatings.

MOFs have garnered significant attention in a broad range of disciplines due to their large accessible surface areas, uniform and tunable pore sizes and chemical modularity.[1] For example, MOFs have been explored for applications to gas adsorption and separation,[2] heterogeneous catalysis,[3] sensor technology,[4] biosciences,[5] and optical devices.[6] Typically, MOFs are synthesized as discrete crystals ranging in size from the nanometers up to millimeters.[2,7] However, for some applications the synthesis of thin films is required. For example, MOF thin films have been employed for the fabrication of optical and electrical devices, such as chemical sensors, fuel cell catalysts and transistors.[8-12] In addition, several of these applications utilize MOF pores to incorporate guest molecules that determine the bulk property of the material.[13] Synthesizing such MOF thin films via a layer-by-layer (LbL) approach allows for the introduction of multi-functionality through judicious choice of organic linkers. Indeed, this has been previously achieved for partially oriented films or crystals where pores with different size and functionality could be realized in a single crystal via epitaxial growth.[14, 15a] These examples of MOF-on-MOF systems showed partial orientation (out-of-plane orientation - order along the axis perpendicular to the interface) because the initial MOF layer, used as a substrate, is only oriented for an out-of-plane direction.[15] A significant advance in this area recently described the synthesis of a centimeter scale polycrystalline MOF film that was aligned in all three crystallographic directions (both in-plane and out-of-plane alignment).[16] Indeed, this work has opened up the possibility of utilizing the anisotropic structural properties of MOFs over commercially relevant scales. Inspired by the opportunity to fill the gap between MOF-on-MOF and precisely oriented MOF films we sought to apply a secondary growth strategy to fabricate fully oriented, multifunctional, copper-based MOF films. In this work we synthesized an oriented MOF film via our recently reported *one pot* method[16] and then employed an LbL (layer-by-layer) approach[17] to grow up two different, epitaxially matched, MOF layers (Figure 1). This strategy enabled MOF-on-MOF films with alignment of all three crystallographic orientations to be synthesized. A salient aspect of this strategy is that it facilitates the synthesis of oriented MOFs from organic linkers that are not compatible with *one pot* epitaxial growth approach. For example, we were unable to grow precisely aligned MOF films on $Cu(OH)_2$ using the bipyridyl functionalized ligand, BPYDC. This is presumably due to the metal-binding properties of the bipyridine moiety interfering with the epitaxial growth mechanism.[18] However, by applying the LbL approach precisely oriented films of $Cu_2(BPYDC)_2$ can be successfully grown as an upper MOF layer. Incorporating a bipyridine linker into the oriented MOF lattice allows for metal to be occluded within the pore structure of the MOF. Thus, the present study provides a strategy for introducing otherwise inaccessible functionality into precisely aligned MOF films.

[a] K. Ikigaki, Dr. K. Okada, Prof. Y. Tokudome, Prof. M. Takahashi,
Department of Materials Science
Osaka Prefecture University
Sakai, Osaka 599-8531, Japan
E-mail: masa@photomater.com
[b] Prof. M. Takahashi, Prof. Y. Tokudome,
International Institute for Nano-Meso Materials Science
Osaka Prefecture University
Sakai, Osaka, 599-8531, Japan
[c] Dr. T. Toyao,
Institute for Catalysis
Hokkaido University
Sapporo, Hokkaido, 001-0021, Japan
[d] Prof. P. Falcalo,
Institute of Physical and Theoretical Chemistry
Graz University of technology
Stremayrgasse 9/Z2, 8010 Graz, Austria
[e] Prof. C. Doonan,
Department of Chemistry
The University of Adelaide
Adelaide, South Australia 5005, Australia

Supporting information for this article is given via a link at the end of the document.((Please delete this text if not appropriate))

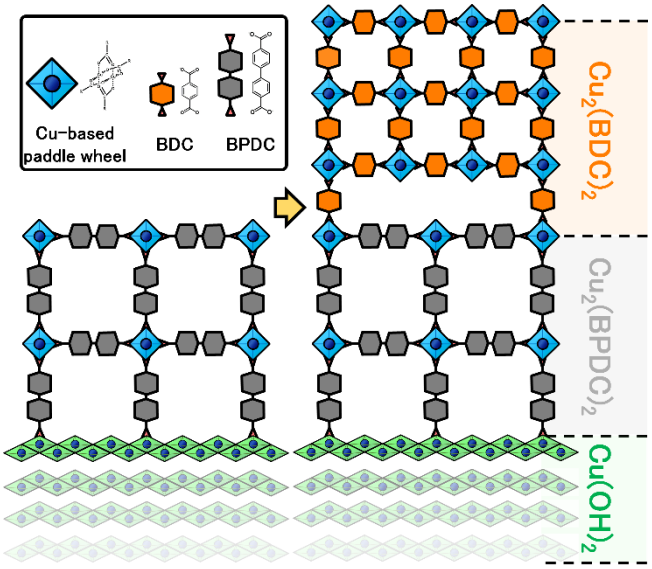

Figure 1. Schematic illustration showing the epitaxial growth strategy of the present study.

Matching of lattice constants is a significant determining factor for the epitaxial growth process.[16,19] For example, epitaxial growth between metal and semiconductor surfaces has been demonstrated at a mismatch of 2.68 %.[19] Indeed, our previous work showed that the growth of heteroepitaxial ceramic-MOF films was limited to a maximum lattice mismatch of 1.8 %.[16] However, for more structurally flexible MOF-on-MOF systems epitaxial growth has been observed for lattice mismatches as large as 20 %.[12b] Based on these previous studies, we employed BPDC as the organic ligand to afford the epitaxial growth of the 2D MOF $Cu_2(BPDC)_2$ on a sacrificial $Cu(OH)_2$ substrate which is composed of oriented copper hydroxides nanobelts (Figure 1). Given the negligible lattice mismatch (SI Fig. 1) we identified $Cu_2(BDC)_2$ as a candidate for a MOF-on-MOF multilayer film.

The secondary, upper, $Cu_2(BDC)_2$ layer was deposited on $Cu_2(BPDC)_2$ using LPE via an LbL approach (described in SI Experimental procedure). The crystallographic orientation of the MOF-on-MOF films was examined by XRD (X-ray diffraction) experiments by measuring the diffraction patterns at three configurations: out-of-plane, in-plane and the azimuthal angle dependence (SI Fig. 2). Only the (00l) peaks resulting from the $Cu_2(BPDC)_2$ and $Cu_2(BDC)_2$ MOF layers is observed in the out-of-plane XRD measurements (Figure 2a and b), indicating that the (00l) faces of both $Cu_2(BPDC)_2$ and $Cu_2(BDC)_2$ are parallel to the substrate. The in-plane XRD measurements were carried out by measuring the diffraction pattern with an X-ray irradiation parallel and perpendicular to the c axis of $Cu(OH)_2$ nanobelts. Close inspection of the data shows that the (010) and both (100) and (200) planes of $Cu_2(BPDC)_2$ and $Cu_2(BDC)_2$ are parallel and perpendicular to the c axis of $Cu(OH)_2$, respectively. These results indicate that the (h00) and (0k0) faces of both the $Cu_2(BPDC)_2$ and $Cu_2(BDC)_2$ layers are aligned orthogonally to each other and perpendicularly to the $Cu(OH)_2$ substrate. This interpretation is supported by the azimuthal angle dependence XRD measurement of the (100) peak of $Cu_2(BPDC)_2$ and $Cu_2(BDC)_2$ and the (002) peak of $Cu(OH)_2$ (Figure 2c), which shows that the maximum intensity in the profiles of the (100) peak of $Cu_2(BPDC)_2$ and $Cu_2(BDC)_2$ is obtained at 90 ^{0} and 270 ^{0} which is the same angle with that of the (002) peak of the $Cu(OH)_2$ nanobelts. The stacking order of $Cu_2(BDC)_2$-on-$Cu_2(BPDC)_2$-on-$Cu(OH)_2$ was confirmed by X-ray incidence angle dependence (SI Fig. 3). These results showed that the secondary (top) $Cu_2(BDC)_2$ layer replicates the crystallographic orientation of the underlying $Cu_2(BPDC)_2$-on-$Cu(OH)_2$ polycrystalline film in both the out-of-plane and in-plane directions. We assessed the morphology of the $Cu_2(BDC)_2$-on-$Cu_2(BPDC)_2$-on-$Cu(OH)_2$ film at each synthetic step via SEM (scanning electron microscopy) (Figure 3). The top-view SEM images of the $Cu_2(BPDC)_2$-on-$Cu(OH)_2$ and the $Cu_2(BDC)_2$-on-$Cu_2(BPDC)_2$-on-$Cu(OH)_2$ film show a distinct change in morphology upon addition of the upper $Cu_2(BDC)_2$ layer that is consistent with the final MOF layer. For example, the teardrop-shaped particles that are characteristic of the previously reported, aligned, $Cu_2(BDC)_2$-on-$Cu(OH)_2$[16] material are observed for the MOF-on-MOF film. Cross-sectional SEM images of $Cu_2(BDC)_2$-on-$Cu_2(BPDC)_2$-on-$Cu(OH)_2$ (SI Fig. 4) show that the film thickness is dependent on the number of LbL cycles until 50, beyond this point crystal growth plateaued.

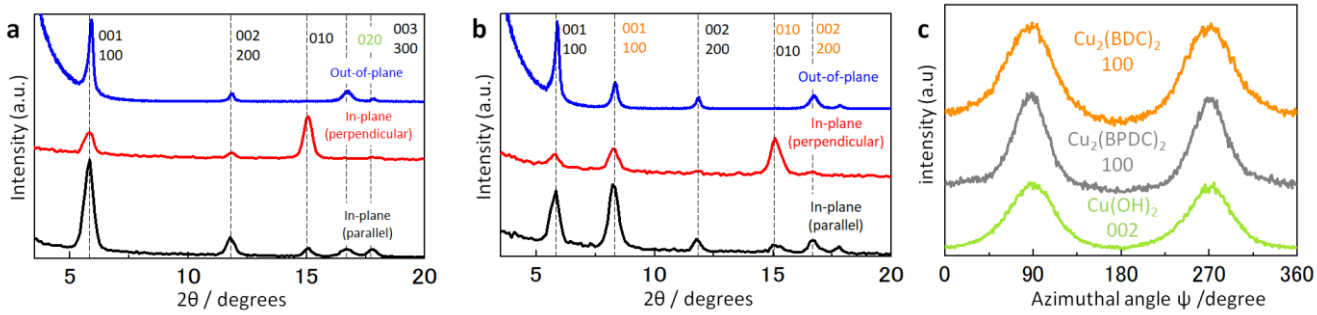

Figure 2. (a) XRD patterns from $Cu_2(BPDC)_2$ epitaxially grown on aligned $Cu(OH)_2$ film; out-of-plane (blue line), in-plane (black and red line, X-ray incident angle is respectively parallel and perpendicular to longitudinal direction of nanobelts at ψ=0 ˚ ,90 ˚). (b) XRD patterns from MOF-on-MOF film of $Cu_2(BDC)_2$ epitaxially grown on aligned $Cu_2(BPDC)_2$ film by an Layer-by-Layer approach. (c) Azimuthal angle dependence of intensity profiles of the (002) reflection of $Cu(OH)_2$ at a diffraction angle of 34.03 and the (100) reflection of $Cu_2(BDC)_2$ and $Cu_2(BPDC)_2$ at a diffraction angle of 8.28˚ and 5.84˚ respectively from $Cu_2(BDC)_2$-on-$Cu_2(BPDC)_2$-on-$Cu(OH)_2$ thin film. Color of hkl in figures indicates diffraction from $Cu_2(BPDC)_2$ (black), $Cu_2(BDC)_2$ (orange), and $Cu(OH)_2$ (green).

We extended the LbL strategy to add an additional, distinct, MOF layer ($Cu_2(NDC)_2$, NDC = naphthalene 2,6-dicarboxylate) to afford an oriented polycrystalline film composed of 3 different MOFs: ($Cu_2(NDC)_2$-on-$Cu_2(BDC)_2$-on-$Cu_2(BPDC)_2$-on-$Cu(OH)_2$). SEM image collected after the addition of a new MOF layer is shown in Figure 3. The SEM images in Fig. 3 clearly show the change in surface morphology that is associated with the addition of each new MOF layer. Furthermore, the structural alignment of this multi-layer film was confirmed by out-of-plane, in-plane and azimuthal angle dependence XRD measurements (SI Fig. 5). The further versatility of this approach was explored by synthesizing multi-layered MOF-on-MOF films composed of different metal nodes, e.g ($Zn_2(BDC)_2$-on-$Cu_2(BDC)_2$-on-$Cu(OH)_2$, and $Co_2(BDC)_2$-on-$Cu_2(BDC)_2$-on-$Cu(OH)_2$) (SI Fig. 6). Once again these MOF-on-MOF films showed complete alignment along all crystallographic directions with respect to the underlying substrate.

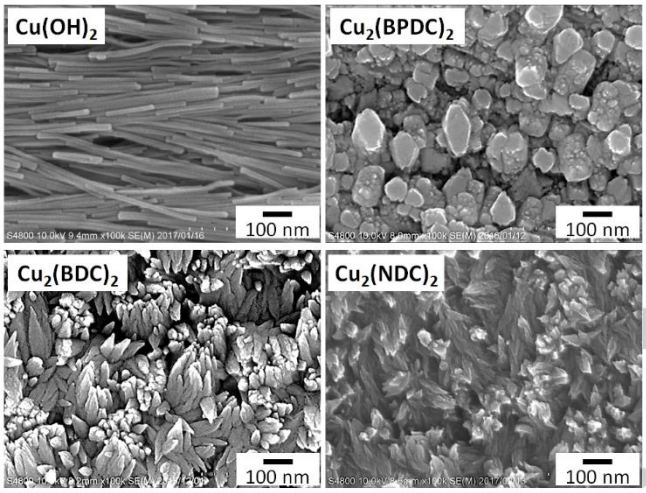

Figure 3. The stepwise SEM images of $Cu_2(NDC)_2$-on-$Cu_2(BDC)_2$-on-$Cu_2(BPDC)_2$-on-$Cu(OH)_2$ thin film.

An advantage of the LbL approach is that it allows for functional groups to be introduced into the oriented MOF-on-MOF films that could not be realized using the one-pot strategy. This is because certain organic linkers can interfere with the epitaxial growth mechanism on $Cu(OH)_2$. For example, the BPYDC ligand, which is extensively used in MOFs to enhance their functionality via post-synthetic metalation,[20] does not afford precisely aligned systems via the one-pot synthesis (SI Fig. 7). This is presumably because the BPYDC ligand can interact with the $Cu(OH)_2$ substrate via both the carboxylate and bipyridine moieties.[18] To demonstrate how the LbL approach can expand the functionality of oriented MOF systems we synthesized a MOF-on-MOF multilayer material, $Cu_2(BPYDC)_2$-on-$Cu_2(BPDC)_2$-on-$Cu(OH)_2$. In this case $Cu_2(BPDC)_2$ was selected as the first layer as it has essentially identical lattice to $Cu_2(BPYDC)_2$. Epitaxial growth of $Cu_2(BPYDC)_2$-on-$Cu_2(BPDC)_2$ was confirmed by comprehensive XRD experiments (SI Fig. 8). We then carried out a post synthetic metalation reaction to incorporate $PdCl_2$ into the upper $Cu_2(BPYDC)_2$ layer (SI Fig. 9). The absorption of $PdCl_2$ within the $Cu_2(BPYDC)_2$-on-$Cu_2(BPDC)_2$-on-$Cu(OH)_2$ film was examined by EDS (energy dispersive X-ray spectroscopy). Inspection of the data (SI Fig. 10) shows that $PdCl_2$ is localized within the upper $Cu_2(BPYDC)_2$ layer. Analogous metalation experiments performed on $Cu_2(BPDC)_2$-on-$Cu(OH)_2$ did not show any evidence that $PdCl_2$ was occluded in the material after washing with fresh acetonitrile. Thus, these results confirm that the chelating bipyridine moiety is required to anchor the metal salts to the framework. Metal ions can be introduced in $Cu_2(BPYDC)_2$ as precursors for metal nanoparticles.[21] This motivated us to generate silver nanoparticles (Ag NPs) in the MOF-on-MOF film and assess their photophysical properties when embedded in an anisotropic lattice. First, we exposed $Cu_2(BPYDC)_2$-on-$Cu_2(BPDC)_2$-on-$Cu(OH)_2$ to Ag^+ ions and then formed Ag NPs by treating the MOF-on-MOF film with 20k bar of H_2 at 80 ˚C (Figure 4).[22]

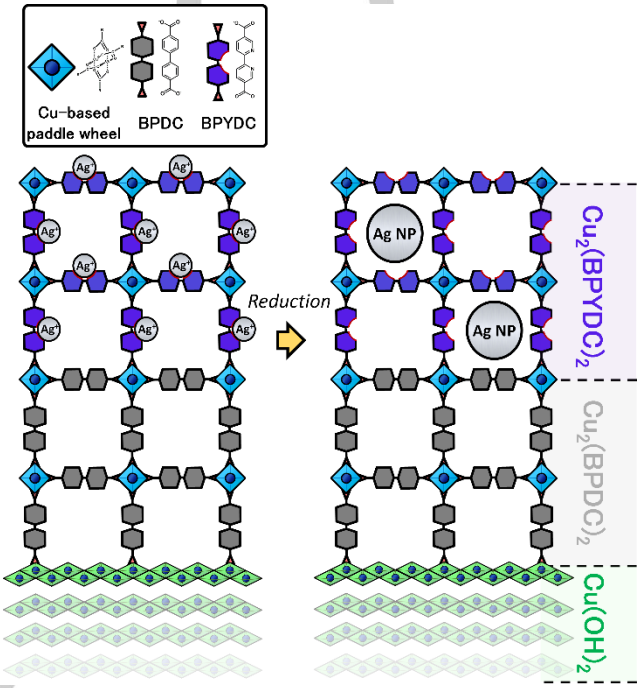

Figure 4. Schematic illustration, showing the experimental concept of formation of Ag NPs-introduced MOF-on-MOF thin film.

The presence of Ag NPs in the MOF-on-MOF film was confirmed by TEM (transmission electron microscopy) and ED (electron diffraction) experiments (SI Fig.11). The spherical Ag NPs possessed an average diameter of 4~5 nm and are distributed in the MOF-on-MOF film without aggregation (SI Fig. 12). Cross sectional STEM (scanning transmission electron microscopy) and the EDS mapping images clearly showed that the Ag NPs were localized dominantly in the upper $Cu_2(BPYDC)_2$ layer (Figure 5a and SI Fig. 13). It should be highlighted that the present oriented MOF film with Ag NPs is one of a few examples where spherical metal nanoparticles are incorporated in an anisotropic lattice.[23] Figure 5b shows the polarization-dependent UV-Vis absorption spectra measured with an integrated sphere in a reflection mode. The difference absorption spectra before and after the Ag NP impregnation are also shown in Figure 5c. We note there are two types of polarization-dependent changes in the plasmon resonance of Ag NPs: plasmon damping and peak shift. This unique optical behavior, for Ag NPs, is likely due to the structural anisotropy of the oriented MOF lattice. For example, the intensity of the Ag NP

plasmon resonance observed at ca. 400-500 nm (Figure 5b) clearly decreases when the angle between the a-axis of MOF and the light polarization increases from 0 ° to 90 °. Furthermore, the maximum intensity of the plasmon resonance was observed when the light polarization is parallel to the a-axis of the $Cu_2(BPYDC)_2$ MOF layer (parallel to the a-c plane of MOF framework linked by Cu-paddlewheel and bi-carboxylates). Previous reports indicated that the damping of plasmon resonance can take place through an electron-phonon interaction.[24] Thus the observed anisotropic plasmon damping may result by anisotropic thermal conductivity (phonon diffusion) in the host MOF matrix as it is expected that for the $Cu_2(BPYDC)_2$ MOF the thermal conductivity is larger along b-axis (pore direction).[25] The observed shift in the plasmon resonance peak to longer wavelengths with increasing angle between light polarization and a-axis of $Cu_2(BPYDC)_2$ can also be explained by the anisotropic nature of the MOF lattice. In this case the shift likely results from dielectric constant anisotropy of MOF matrix[26] as it is well-known that plasmon resonance wavelengths are longer when metal nanoparticles are accommodated in a matrix with larger dielectric constants.[27] The precise alignment of this MOF-on-MOF system allows for the plasmon resonance of guest Ag NPs to be modulated by changing the orientation of the MOF thin film. Accordingly, the present results show that MOF-on-MOF films can be used to generate an anisotropic response from functional moieties aligned within their pores.

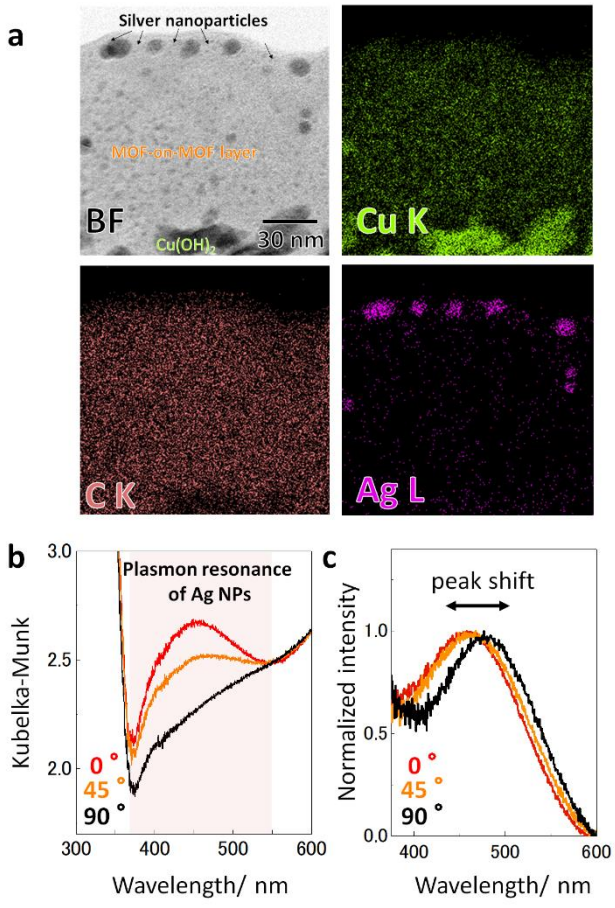

Figure 5. (a) Cross sectional STEM and EDS mapping images of $Cu_2(BPYDC)_2$-on-$Cu_2(BPDC)_2$ layer grown on $Cu(OH)_2$ nanobelts containing Ag NPs. (b) Polarization-dependent UV-Vis reflection spectra of the MOF-on-MOF films with Ag NPs. Angles in the figure show the angles between a-c plane of MOF crystal (Cu-paddle wheel sheet) and electric field component of polarization of the light, respectively. (c) Difference absorption spectra of before and after Ag NP impregnation (intensity is normalized to the peak maximum).

Herein, we prepared precisely aligned MOF-on-MOF thin films composed of up to three different MOF layers, via a *one pot* heteroepitaxial growth strategy (bottom MOF layer) followed by an LbL approach (for subsequent MOF layers). Comprehensive XRD analysis confirmed that each MOF layer was heteroepitaxially matched and aligned to the $Cu(OH)_2$ substrate in all three crystallographic directions. By employing the LbL approach we were able to fabricate multilayer MOF-on-MOF films that included BPYDC, an organic linker that could not form an aligned MOF via the one-pot method. Furthermore, we demonstrated that $Cu_2(BPYDC)_2$-on-$Cu_2(BPDC)_2$-on-$Cu(OH)_2$ could occlude Ag NPs within its aligned pore network and engender orientation dependent plasmon resonance. Accordingly, this work represents a strategy for synthesizing multifunctional materials that allow for anisotropic properties of functionalized organic linkers and pore guest species. It is anticipated that aligned MOF-on-MOF films will find applications to areas of technology, such as optical, thermal, electronic and magnetic devices where precise control of structure and atomic positions is highly desired.

Experimental section

Experimental procedures were described in supporting information.

Acknowledgement

The present work is partially supported by JSPS KAKENHI. Prof. Koichi Okamoto of OPU and Prof. Jorge Pérez Juste of University of Vigo are greatly appreciated for fruitful discussion on the anisotropic plasmon resonances. P.F. acknowledges TU Graz for the Lead Project (LP-03) and the European Union's Horizon 2020 Programme (FP/2014-2020)/ERC Grant Agreement n.771834 −POPCRYSTAL. CJD acknowleges the JSPS visiting professor scheme.

Keywords: metal-organic frameworks • crystal growth • heteroepitaxial growth • microporous materials • mof-on-mof

[1] H. Furukawa, K. E. Cordova, M. O'Keeffe, O. M. Yaghi, *Science*. **2013**, 30, 1230444.

[2] M. Eddaoudi, J. Kim, N. Rosi, D. Vodak, J. Wachter, M. O'Keeffe, O. M. Yaghi, *Science*. **2002**, 18, 469-472.

[3] J. Y. Lee, O. K. Farha, J. Roberts, K. A. Scheidt, S. T. Nguyen, J. T. Hupp, *Chem. Soc. Rev*. **2009**, 38, 1450-1459.

[4] a) L. E. Kreno, K. Leong, O. K. Farha, M. Allendorf, R. P. Van Duyne, J. T. Hupp, *Chem. Rev*. **2012**, 112, 1105-1125. b) J. E. Mondloch, M. J. Katz, W. C. Isley, P. Ghosh, P. Liao, W. Bury, G. W. Wagner, M. G. Hall, J. B. DeCoste, G. W. Peterson, R. Q. Snurr, C. J. Cramer, J. T. Hupp & O. K. Farha, *Nat. Mater*. **2015**, 14, 512-516.

[5] C. Doonan, R. Riccò, K. Liang, D. Bradshaw, P. Falcaro, *Acc. Chem. Res.* **2017**, 50, 1423-1432.

[6] M. D. Allendorf, C. A. Bauer, R. K. Bhaktaa R. J. T. Houk, *Chem. Soc. Rev.* **2011**, 112, 1330-1352.

[7] S. Han, Y. Wei, C. Valente, I. Lagzi, J. J. Gassensmith, A. Coskun, J. F. Stoddart, B. A. Grzybowski, *J. Am. Chem. Soc.* **2010**, 132, 16358-16361.

[8] I. Stassen, N. Burtch, A. Talin, P. Falcaro, M. Allendorfc, R. Ameloot, *Chem. Soc. Rev.* **2017**, 46, 3185-3241.

[9] P. Falcaro, R. Ricco, C. M. Doherty, K. Liang, A. J. Hill, M. J. Styles, *Chem. Soc. Rev.* **2014**, 43, 5513-5560.

[10] S. Furukawa, J. Reboul, S. Diring, K. Sumida, S. Kitagawa, *Chem. Soc. Rev*. **2014**, 43, 5700-5734.

[11] M.-D. Allendorf, A. Schwartzberg, V. Stavila, A.-A. Talin, *Chem. Eur. J.* **2011**, 17, 11372-11388.

[12] O. Shekhah, J. Liu, R. A. Fischer, and C. Wöll, *Chem. Soc. Rev.* **2011**, 40, 1081-1106.

[13] V. Stavila, A. A. Talin and M. D. Allendorf, *Chem. Soc. Rev.* **2014** 43, 5994-6010.

[14] O. Shekhah, K. Hirai, H. Wang, H. Uehara, M. Kondo, S. Diring, D. Zacher, R. A. Fischer, O. Sakata, S. Kitagawa, S. Furukawa, C. Wöll, *Dalton Trans.* **2011**, 40, 4954-4958.

[15] a) S. Furukawa, K. Hirai, Y. Takashima, K. Nakagawa, M. Kondo, T. Tsuruoka, O. Sakata, S. Kitagawa, *Chem. Commun.* **2009**, 5097-5099. b) Z. Wang, J. Liu, B. Lukose, b) Z. Gu, P. G. Weidler, H. Gliemann, T. Heine, C. Wöll, *Nano Lett.* **2014**, 14, 1526-1529. c) V. Chernikova, O. Shekhah, I. Spanopoulos, P. N. Trikalitis, M. Eddaoudi, *Chem. Commun.* **2017**, 53, 6191-6194.

[16] P. Falcaro, K. Okada, T. Hara, K. Ikigaki, Y. Tokudome, A. W. Thornton, A. J. Hill, T. Williams, C. Doonan, M. Takahashi, *Nature Mater.* **2017**, 16, 342-348.

[17] O. Shekhah, H. Wang, S. Kowarik, F. Schreiber, M. Paulus, M.Tolan, C. Sternemann, F. Evers, D. Zacher, R. A. Fischer, C. Wöll, *J. Am. Chem. Soc.* **2007**, 129, 15118-15119.

[18] S. M. Barnett, K. I. Goldberg, J. M. Mayer, *Nat. Chem.*, **2012**, 4, 498-502.

[19] F. R. Fan, Y. Ding, D. Y. Liu, Z. Q. Tian, Z. L. Wang, *J. Am. Chem. Soc.,* **2009**, 131, 34, 12036-12037

[20] a) J. D. Evans, C. J. Sumby, C. J. Doonan, *Chem. Soc. Rev*. **2014**, 43, 5933-5951. b) E. D. Bloch, D. Britt, C. Lee, C. J. Doonan, F. J. U-Romo, H. Furukawa, J. R. Long, O. M. Yaghi, *J. Am. Chem. Soc*. **2010**, 132, 14382-14384.

[21] P. Falcaro, R. Ricco, A. Yazdi, I. Imaz, S. Furukawa, D. Maspoch, R. Ameloot, J. Evans, C. J. Doonan, *Coordination Chemistry Reviews,* **2016**, 307, 237-254.

[22] a) J. L. C-Huaman, K. Sato, S. Kurita, T. Matsumotoc, B. Jeyadevan, *J. Mater. Chem.* **2011**, 21, 7062-7069. b) D. D. Evanoff, Jr., G. Chumanov, *J. Phys. Chem. B*, **2004**, 108, 37, 13949.

[23] J. Han, P. Fang, W. Jiang, L. Li, R. Guo, *Langmuir,* **2012**, 28, 4768−4775.

[24] a) K. Okamoto, M. Funato, Y. Kawakami, K. Tamada, *J. Photochem. Photobiol.C: Photochem. Rev.,* 2017, 32, 58-77. b) A. Melikyan, H. Minassian, *Appl. Phys. B,* **2004**, 78, 454-455. c) T. G. Habteyes, S. Dhuey, E. Wood, D. Gargas, A. Cabrini, P. J. Schuck, A. P. Alivisatos, S. R. Leone, *ACS NANO*, **2012**, 6, 5702-5709.

[25] X. Wang, R. Guo, D. Xu, J. D. Chung, M. Kaviany, B. Huang, *J. Phys. Chem*. C **2015**, 119, 26000−26008.

[26] A. Choudhary, L. Guoqiang, *Optics Express*, **2014**, 22, 24348–24357.

[27] M. B. Cortie, A. M. McDonagh, *Chem. Rev.,* **2011**, 111, 6, 3713-3735.

Entry for the Table of Contents (Please choose one layout)

Layout 1:

COMMUNICATION

Text for Table of Contents

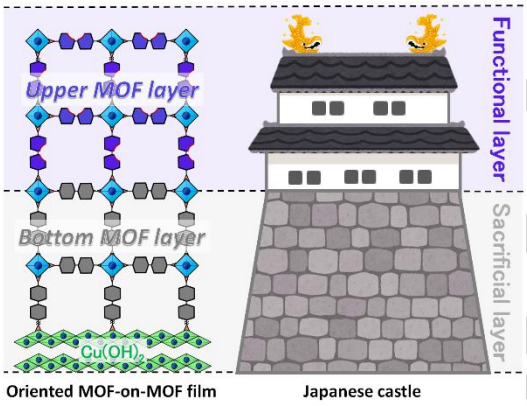

Ken Ikigaki, Kenji Okada, Yasuaki Tokudome, Takashi Toyao, Paolo Falcaro, Christian Doonan, and Masahide Takahashi**

Page No. – Page No.

Oriented growth of multiple layered thin films of metal-organic frameworks (MOF-on-MOF)